EFFECTS OF CLIMATE WARMING ON DISSOLVED OXYGEN CONCENTRATIONS IN LAKE ERIE

ALAN F. BLUMBERG AND DOMINIC M. DI TORO

Made in United States of America
Reprinted from TRANSACTIONS OF THE AMERICAN FISHERIES SOCIETY
Vol. 119, No. 2, March 1990

Transactions of the American Fisheries Society 119:210–223, 1990

Effects of Climate Warming on Dissolved Oxygen Concentrations in Lake Erie

ALAN F. BLUMBERG AND DOMINIC M. DI TORO

HydroQual, Inc.
1 Lethbridge Plaza, Mahwah, New Jersey 07430, USA

Abstract.—A coupled hydrodynamic and water quality model was used to examine the response of dissolved oxygen concentrations to warming of the central basin of Lake Erie. An area-averaged hydrodynamic model was used to estimate the lake temperatures and thermocline variability as forced by surface heating and winds. Vertical turbulence mixing processes were incorporated by a second-moment, turbulence closure submodel. The water quality model comprised a set of 15 mass balance equations that predicted distributions of phytoplankton biomass, nutrient concentration, and dissolved oxygen. A synthesis of the results from the coupled model forced by climate warming scenarios from three atmospheric general circulation models suggested that there will be a substantial decline in oxygen concentrations in the central basin. Although forecasts of future conditions that are beyond established experiences are uncertain, it appears likely that climate warming will lead to such a decline regardless of details in changes of lake stratification dynamics. Losses of 1 mg/L of dissolved oxygen in the upper layers and of 1–2 mg/L in the lower layers of Lake Erie's central basin can be expected, along with an increase in the area of the lake that is anoxic. The decline in dissolved oxygen is predicted to be due to warmer lake temperatures, which increase the rate of bacterial activity in the hypolimnion waters and sediment, rather than to thermocline location and volume of water below the thermocline.

Atmospheric accumulations of greenhouse gases, of which carbon dioxide is the major constituent, have led to concern that the earth's climate may be undergoing a global warming as a result. If current trends in the emissions of these gases continue, the earth could experience a global mean warming of 2.8–4.2°C in the next century or so (Schlesinger and Mitchell 1987). It becomes important to identify and quantify the potential effects of climatic change so that alternatives may be developed to cope with such warming. Our study seeks to determine how climate warming will affect water quality in Lake Erie. The conclusions of this study, while specific to the central basin of Lake Erie, have implications for the other Great Lakes, especially for embayments and nearshore areas.

Water quality in Lake Erie has been sensitive to human interference. The nutrient inputs to all the Great Lakes, and to Lake Erie in particular, increase the production of algal biomass (Vollenweider et al. 1980). Formation of a thermocline isolates the hypolimnion and dissolved oxygen concentration decreases due to algal respiration. If algal abundance is excessive, anoxic conditions fatal to aerobic organisms, including fish, result. Because the joint U.S.–Canada agreement on Great Lakes water quality chose the elimination of anoxia as the goal for phosphorus control in Lake Erie (IJC 1978), we use changes in dissolved oxygen as the measure of changes in overall water quality.

The consequences of climatic warming and increased atmospheric temperature may be dramatic in lakes because changes in surface heating can affect stratification. The extent of oxygen depletion depends on several factors, an important one being thermocline depth. If the thermocline is established nearer the surface, the volume of water in the hypolimnion is increased and more oxygen is available. However, establishment of the thermocline nearer the bottom reduces hypolimnion volume and oxygen depletion will occur sooner. The actual occurrence of anoxia is a balance between the rate of oxygen depletion and lake destratification in autumn. Warmer lake temperatures could also lead to anoxia or hypoxia by increasing the metabolic rate of sediment bacteria and biological productivity and respiration in the water column, and by decreasing dissolved oxygen saturation values. Thus, the reduction in the areal extent and occurrence of anoxia that has been achieved by expensive phosphorus control measures (IJC 1978) may be reversed by a systematic warming trend.

Data collected from 1970 and 1975 in the central basin of Lake Erie form the basis for much of this study. These years are referred to as the base years. In terms of water quality, the two years were quite different: there was considerable anoxia in

the deeper portions of the lake in 1970 but none in 1975. Another important difference between 1975 and 1970 was the shallow depth of the thermocline in 1975. Use of these two years made possible the direct application of a Lake Erie eutrophication model that has been calibrated and verified for these years. The use of different years in our analysis probably would not change the conclusions of our study because 1970 and 1975 bracket the range of possible conditions with respect to dissolved oxygen. However, these years do not represent a full range of climatic, hydrological, or chemical loading variability.

Methods

Two existing, well-tested, modeling frameworks were used in the analysis. To estimate water temperatures and thermocline variation produced by climatic changes, a hydrodynamic model of the central basin of Lake Erie was constructed. The vertical temperature distributions estimated by this model were then used in a calibrated water quality—more specifically, eutrophication—model of Lake Erie through the use of a consistent model coupling procedure. Three climatic change scenarios developed from atmospheric general circulation model simulations performed by Hansen et al. (1984) at the Goddard Institute for Space Studies (GISS), Manabe and Wetherald (1986) at the Geophysical Fluid Dynamics Laboratory (GFDL), and Schlesinger and Zhao (1988) at Oregon State University (OSU) were used with the two models to examine relationships between climate changes and water quality.

Hydrodynamic Model

The most important cause of motion and mixing in a lake is the surface wind. In summer, under stable thermal stratification, vertical mixing due to winds is usually limited to the surface layers. In narrow lakes, currents in surface layers parallel the wind. Below the surface wind-mixed layer, there is a compensating and oppositely directed current. In wide lakes, the structure of surface currents and deep compensating flows is more complex and considerably modified by depth variations. Strong, persistent winds or weak vertical stability result in a gradual increase in the thickness of the wind-mixed layer, and wind-induced currents are spread over a larger portion of the water column. One can estimate vertical distributions of currents, turbulent mixing, and bottom stress from a knowledge of surface wind stress in conjunction with a one-dimensional (vertical direction) hydrodynamic model.

Many one-dimensional models have been developed for predicting vertical temperature distributions and mixed layer depths. Lam and Schertzer (1987) and McCormick and Meadows (1988) performed calculations for Lake Erie with a variety of these models, all of which have yielded good estimates of the various computed quantities. The disadvantage of all the models used in those two studies is that they are one-problem models whose constants are adjusted for the specific application and time periods under consideration. Their calculations are quite dependent on an existing data base, so they lack universality; they typically cannot be exercised beyond the range of the data for which they were developed. On the other hand, the model we use here has had its constants determined from laboratory turbulence data and can cope with a fairly broad range of turbulence problems and attendant forcing functions. Furthermore, it has been demonstrated (Mellor and Yamada 1982; Galperin et al. 1988) that the model does well in simulating a wide range of engineering and geophysical problems, including a suite of laboratory fluid flow experiments. In all of the tests, arbitrary adjustment of the model's nondimensional constants has not been required. The linearized, area-averaged, governing equations are

$$A\frac{\partial U}{\partial t} - fVA = \frac{\partial}{\partial z}\left[A(K_M + \nu)\frac{\partial U}{\partial z}\right] + \frac{\Delta(\mathrm{BP})_x}{\rho_o}, \tag{1}$$

$$A\frac{\partial V}{\partial t} + fUA = \frac{\partial}{\partial z}\left[A(K_M + \nu)\frac{\partial V}{\partial z}\right] + \frac{\Delta(\mathrm{BP})_y}{\rho_o}, \tag{2}$$

and

$$A\frac{\partial \theta}{\partial t} = \frac{\partial}{\partial z}\left[A(K_H + \nu)\frac{\partial \theta}{\partial z}\right]; \tag{3}$$

z and t are the vertical space coordinate and time, respectively; $A(z)$ is the horizontal area; U and V are the velocities in the east–west and north–south directions, respectively; θ is temperature, and ρ_o is fluid density. The surface-compensating return flow at depth is produced through the right-most terms in equations (1) and (2), in which $\Delta(\mathrm{BP})$ is the difference in pressure between the east and west (north and south) ends of the basin integrated along the respective north–south (east–west) end boundaries. These pressure terms are obtained by

appealing to the steady form of the vertically integrated continuity equations, which imposes the condition that the vertical integrals of U and V vanish. Use of the steady form involves the assumption that both the surface gravity and internal waves generated by the end boundaries instantaneously propagate to the center of the basin and set up the lake surface and thermocline. Currents that occur on time scales greater than a day or so are thus properly accounted for, whereas higher-frequency motions are not.

The vertical turbulent mixing coefficients for momentum and heat in equations (1)–(3), K_M and K_H, are computed from the turbulence closure submodel of Mellor and Yamada (1982). This submodel contains nondimensional empirical constants that are fixed by reference to a small subset of the available laboratory data and are independent of particular hydrodynamic model applications. A background mixing, to account for internal waves and other unresolved physical processes, is denoted as ν, equal to 0.01 cm^2/s and applied uniformly in all of the calculations. Boundary conditions at the surface are

$$\rho_o(K_M + \nu)\left[\frac{\partial U}{\partial z}, \frac{\partial V}{\partial z}\right] = \left[\tau_x^w, \tau_y^w\right] \quad (4)$$

and

$$(K_H + \nu)\frac{\partial \theta}{\partial z} = Q; \quad (5)$$

at the bottom, they are

$$\rho_o(K_M + \nu)\left[\frac{\partial U}{\partial z}, \frac{\partial V}{\partial z}\right] = \left[\tau_x^b, \tau_y^b\right] \quad (6)$$

and

$$(K_H + \nu)\frac{\partial \theta}{\partial z} = 0; \quad (7)$$

τ^w and τ^b denote surface wind stress and bottom frictional stress; Q denotes surface heat flux; and the subscripts x and y denote components in the easterly and northerly directions.

No heat transfer to the sediments is permitted by the use of equation (7), although such a heat transfer can have a significant effect on near-bottom temperatures of shallow lakes (Heinrich et al. 1981). The process of heat transfer between sediments and overlying waters is poorly understood and therefore is not considered here. The bottom stress is obtained by matching the computed near-bottom velocity to that of the logarithmic law of the wall. This approach for deducing currents, mixing, and bottom stresses has been used successfully many times (e.g., Kraus 1977; Martin 1985). A variation of this approach, whereby the temperature structure is computed but the details of the velocity field are not, has been successfully used in Lake Erie by Lam and Schertzer (1987). For details of the numerical solution technique used here, see Blumberg and Mellor (1983, 1987).

Lake Erie Eutrophication Model

The Lake Erie eutrophication model (Di Toro 1980; Di Toro and Connolly 1980) comprises a set of mass balance equations that quantify the mass transport and kinetic interactions of the biota (phytoplankton and zooplankton) and nutrients (phosphorus, nitrogen, and silica), and compute the resultant concentrations of dissolved oxygen. The model has also been used in more detailed examinations of phosphorus availability (De Pinto et al. 1986). Similar models have been developed and applied to other Great Lakes settings (Thomann et al. 1975; Bierman 1976; Lam et al. 1983). Di Toro et al. (1987) presented a retrospective analysis of the Lake Erie model performance over a 10-year period. That analysis further supported the model's predictive capability.

The eutrophication model was based upon segmentation of Lake Erie into volumes that represent the epilimnion, the hypolimnion, and an active sediment layer of the three major basins (Figure 1). The thickness of the lake layers was determined from estimates of the depth of the summer thermocline (average thermocline depth over the whole summer period). The active sediment layer was explicitly included to account for sediment oxygen demand. The kinetics employed were designed to simulate the annual cycle of phytoplankton production, its relation to the supply of light and available nutrients, and the effect on dissolved oxygen. The calculation was based on a formulation of the kinetics that govern the interactions of the biota and the nutrients, and application of these kinetics to the regions of Lake Erie within the context of equations of conservation of mass. The 15 variables for which these calculations were performed were

phytoplankton
- (1) diatom chlorophyll *a*
- (2) non-diatom chlorophyll *a*

zooplankton
- (3) herbivorous zooplankton carbon
- (4) carnivorous zooplankton carbon

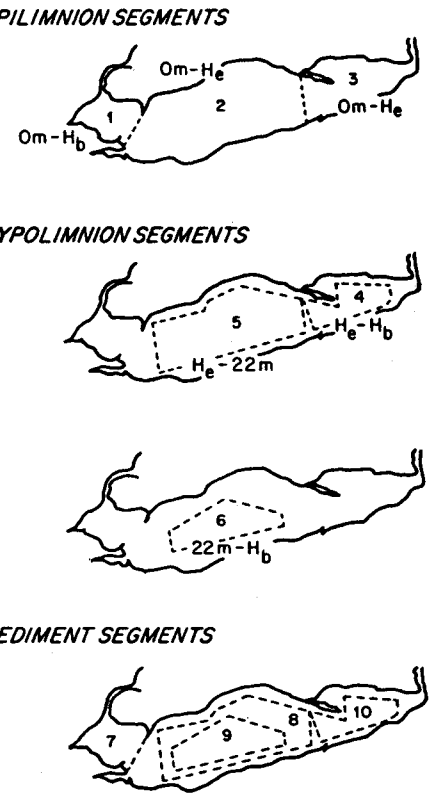

FIGURE 1.—Model segmentation of western, central, and eastern basins of Lake Erie. Water segments are numbered 1–6, sediment segments 7–10. Depths refer to the thickness of the segment; H_e is the thickness of the epilimnion from the surface (0 m) and H_b is the total depth of the water column. Sediment segments are all 5 cm deep.

nitrogen
(5) detrital and dissolved organic nitrogen
(6) ammonia nitrogen
(7) nitrate nitrogen
phosphorus
(8) unavailable phosphorus
(9) soluble reactive phosphorus
silica
(10) unavailable silica
(11) soluble reactive silica
carbon, hydrogen, oxygen
(12) detrital organic carbon
(13) dissolved inorganic carbon
(14) alkalinity
(15) dissolved oxygen.

Comparisons of the model results with extensive field data from 1970 and 1975 (Di Toro and Connolly 1980) demonstrated that the calculation reproduced the major features of the seasonal distribution of phytoplankton and nutrients over a range of observed concentrations. That the western, central, and eastern basin distributions were all reasonably well reproduced by use of the same kinetic structure and coefficients suggested that the calculation has a certain generality and can reproduce conditions as distinct as those in the western and eastern basins.

Hydrodynamic–Eutrophication Model Interaction

To use the eutrophication model in a predictive mode for the analysis of the three climate scenarios, three ingredients were required. The first was the expected water temperatures because of their influence on kinetic rates in the eutrophication model. The second was the depth of the summer thermocline and, hence, the volumes of the epilimnion and hypolimnion. The third was the bulk vertical dispersive exchange between the epilimnion and the hypolimnion. The first two of these ingredients were extracted directly from the hydrodynamic model results. The dispersive exchange was computed by use of the temperature fields from the hydrodynamic model, averaged over the epilimnion and the hypolimnion, in conjunction with a temperature balance equation similar to equation (3) but structured for a two-layer system.

The area integration of equation (3) over the hypolimnion gives

$$V_H \frac{\partial \theta_H}{\partial t} = A_i K_i \frac{\partial \theta_i}{\partial z}; \qquad (8)$$

V_H and θ_H are the volume and the volume-averaged temperature of the hypolimnion, respectively; i denotes the interface between the epilimnion and the hypolimnion. The interfacial dispersion coefficient, K_i, is readily computed from equation (8), given the results of a hydrodynamic model simulation.

Climate Scenarios

In our study, results derived from three simulations of the changes in the equilibrium induced by a doubling of atmospheric CO_2 concentration have been acquired by use of atmospheric general circulation models. Climate scenarios in the form of monthly averaged data over an annual cycle were obtained from Hansen et al. (1984; GISS), Manabe and Wetherald (1986; GFDL), and Schlesinger and Zhao (1988; OSU). The relevant data from each model were selected from that model's grid point closest to Lake Erie. The results of con-

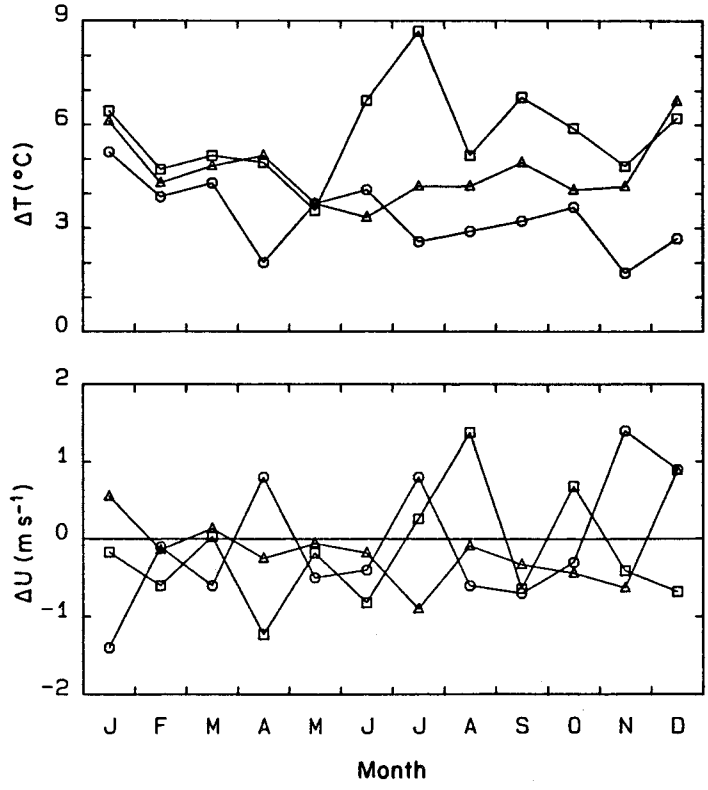

FIGURE 2.—Simulated monthly changes (differences from present-day values) in surface air temperature (ΔT) and vector-averaged wind speed (ΔU) over Lake Erie predicted by three climate models (GISS △; GFDL □; OSU ○), based upon a doubling of atmospheric carbon dioxide.

trol simulations based upon present-day CO_2 concentration were also provided. The differences between the doubled-CO_2 and control climates represent the CO_2-induced changes in the equilibrium climate.

We used monthly-mean differences in surface air temperature and surface wind speed for the climate change calculations (Figure 2). Temperature differences from the GISS and GFDL scenarios (Figure 2) were similar except in June and July when GFDL values were double those of GISS. Both model simulations showed average monthly surface temperatures ranging from 3 to 8°C greater than the control simulations. Contrarily, the OSU scenario exhibited less temperature change (about half of GISS and GFDL results) that ranged from 2 to 5°C above the control simulation.

The wind data available in files for the atmospheric circulation model were vector mean wind speeds instead of the more appropriate scalar mean wind speeds. Vector mean speeds are often significantly less than mean wind speeds and thus can underestimate wind-induced mixing. This error was reduced somewhat here because the winds from the atmospheric models exhibit little directional variability. Changes in wind speed for the doubled-CO_2 scenarios (Figure 2) were small and typically negative. This suggests that winds will weaken under the various climate scenarios. The OSU scenario had higher winds in the critical spring and summer periods, with increases of about 1 m/s.

The heat fluxes and wind stresses required as input by the hydrodynamic model were computed according to

$$Q = Q_o + \frac{\partial Q}{\partial T}\Delta T \tag{9}$$

and

$$\tau = \tau_o + \frac{\partial \tau}{\partial W}\Delta W; \tag{10}$$

Q is heat flux, as before; τ is wind stress; T is air–lake temperature difference; W is wind speed. The o subscript denotes the base year (1970 or 1975), and Δ denotes the difference between the doubled-CO_2 and control climates. The rate of change of

heat flux Q from the lake with respect to the air–lake temperature difference has been computed by Gill (1982), based on the ideas of Haney (1971) for the world ocean. It appears that a value of 32 W/m^2 is appropriate for the latitude of Lake Erie. The rate of change of wind stress with respect to wind speed was estimated to be 3×10^{-3} g/(cm^2·s); a quadratic drag law and a drag coefficient of 1.2×10^{-3} were assumed.

Results and Discussion

Verification of the Hydrodynamic Model

The hydrodynamic model presented above was applied to Lake Erie for the years 1970 and 1975. All simulations started April 1 and ended December 31 to avoid consideration of the extensive ice cover that normally occurs during January through March. There are 40 vertical levels in the model, with finer spacing near the surface than in the deeper regions. A time step of 30 min was used. The model was forced by hourly estimates of surface wind stress and monthly estimates of surface heat flux. A continuous series of hourly wind speed and direction observations for 1970 and 1975 were obtained at the Erie, Pennsylvania, and the Cleveland, Ohio, airports. These observations were corrected from overland to overwater winds (Schwab 1978; Schwab and Morton 1984) and turned into wind stresses by use of a quadratic drag law and a drag coefficient (Large and Pond 1981). Surface heat fluxes were calculated by Di Toro and Connolly (1980) for 1970 and 1975 on a monthly basis by use of heat storage estimates. These values, linearly interpolated to the model time step, were consistent with (although about 5% higher than) those computed by Derecki (1976) and Schertzer (1987) based on hydrometeorological data. The initial temperature profile (April 1) was a vertically homogeneous 2°C.

The predicted temperatures averaged over the epilimnion and hypolimnion fell within the envelope of the observations (mean ± SD) for the most part throughout the annual cycle (Figure 3). The model missed the onset of stratification by a month or so in 1970, but predicted it correctly in 1975. Temperatures in the hypolimnion were not as well predicted as those in the epilimnion. In early summer 1970, for example, the model-predicted temperatures were inaccurate by 2–3°C. The peak in hypolimnion temperature that occurs in September–October, well after the surface peak temperatures, was modeled quite well. The rapid deepening of the epilimnion in autumn due to surface cooling and convection was also predicted by the model. However, the model predicted this overturn event occurred 2–3 weeks later than it actually did. The model appeared to reproduce the maximum stratification in both years. In 1970, data for August (typically the month of greatest stratification) showed bottom and surface temperatures of 11 and 22°C, respectively (ΔT = 11°C). The 1970 model values were 12 and 24°C (ΔT = 12°C). In 1975, the data for the same month showed bottom and surface temperatures of 13 and 22°C (ΔT = 9°C); the 1975 model values were 13 and 20°C (ΔT = 7°C). Thus, although the model was not perfect, it reproduced the quantities most important for assessing the thermal response of the lake to climate warming in that it captured most of the large observed top-to-bottom temperature differences and it did so at the proper time of the year.

The model was also verified by comparing vertical profiles between prediction and observation (Figure 4). The model reproduced the vertical structure observed in 1970, but produced bottom temperatures that were about 3°C warmer than the data, perhaps because there was no mechanism in the model to transfer heat to the sediment. The 1975 comparison, however, indicated substantial discrepancies between data and model output. June 1975 was a transitional period when the vertically mixed lake became stratified. Errors in timing the onset of stratification can lead to the kinds of deviation indicated for 1975. The summer mixed layer was shallow due to intense solar heating and typically weak winds, but deepened rapidly in the fall (upper portion of Figures 5, 6). Isotherms deepened slowly in spring and summer due to downward diffusion, and rose rapidly in fall due to convection and wind mixing.

To improve the difference between the observed and computed thermal structure, one must look toward improving model physics and assembling better model-forcing data. Although some improvements in the exchange processes between the water column and the sediment have been identified, the model physics based on areally averaged dynamics have been well established for basin-wide problems. On the other hand, the data available for model forcing, especially the wind fields and surface heat fluxes, were subject to considerable uncertainty. Midbasin wind stresses were estimated from observations of wind speed and direction at weather stations around the lake. Some of the model error in this study was probably due to the use of only two such stations. Because the

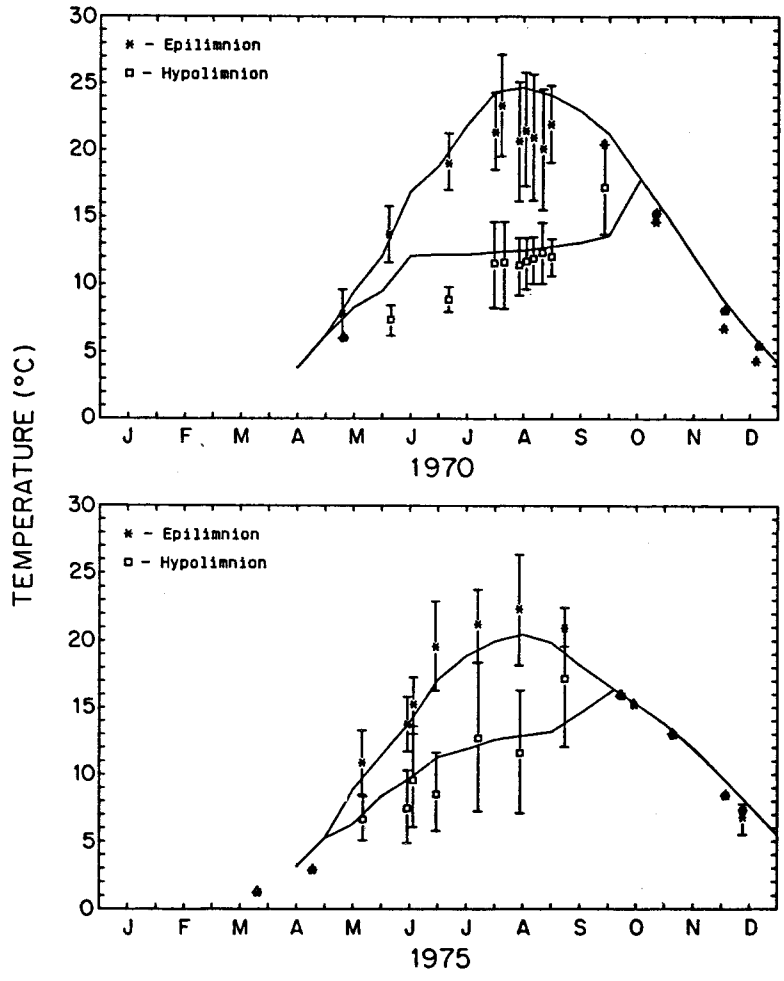

FIGURE 3.—Predicted (solid lines) and observed epilimnion (*) and hypolimnion (□) temperatures for the 1970 and 1975 base conditions. Data are plotted as averages over the epilimnion and hypolimnion ± 1 SD.

timing of the formation and subsequent destruction of the thermocline depended on details in the wind field, the use of perhaps six stations (Lam and Schertzer 1987; Schertzer 1987) around the lake would be necessary to incorporate the spatial variability of the wind fields into the midbasin average. Another source of error has to do with forcing from surface heating. In our analysis, the heat fluxes used in the hydrodynamic model were linearly interpolated between monthly mean values. During the May–June and October–November periods, the heat flux exhibits considerable variability on daily time scales (Schertzer 1987). Significant departures can occur between the daily values and their corresponding monthly means, and this may be contributing to errors in the model.

Thermal Response to Scenarios

The hydrodynamic model was run with the climate-warming scenarios presented earlier. The doubled-CO_2 scenarios produced a warmer and longer-lasting warming regime in the lake (Figures 5, 6) than the base years. The warming season, as defined by the presence of surface water of 18°C or warmer, lengthened by about 40 d over 1970 base conditions and by about 70 d with respect to 1975 base conditions (Table 1). Moreover, the scenarios began warming some 4 weeks earlier and warmed 6 weeks longer with respect to the 1975 base, but about 2 weeks earlier and 2 weeks longer with reference to the 1970 base. The maximum surface temperature increased by about 5°C in all scenarios (Table 1).

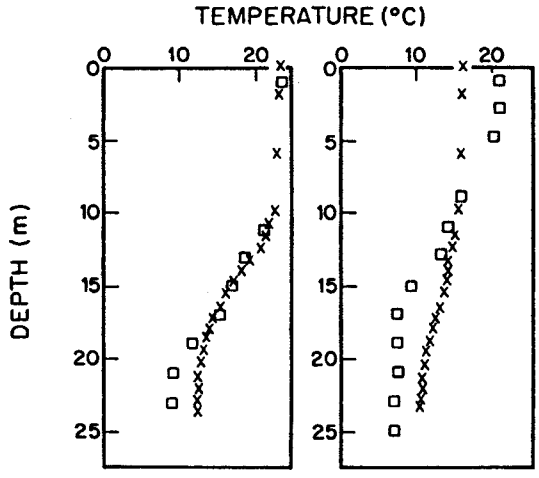

FIGURE 4.—Comparison of predicted and observed thermal vertical structure in the central basin of Lake Erie. Squares are observed data for July 28–29, 1970 (left), and June 24–29, 1975 (right). Crosses are hydrodynamic model predictions.

The thermocline, defined as the depth of the maximum vertical temperature gradient during August (warmest month) became shallower by about 2 m in the GISS and GFDL scenarios. The OSU scenario produced a slightly deeper thermocline than the other two in spite of its smaller air temperature change, apparently because its greater wind speeds mixed the extra surface heating deeper into the water column. Because of the shape of the central basin, a 1–2-m rise in the thermocline led to a 50–100% increase in hypolimnion volume (Table 1). The 1975-based OSU scenario with its deeper thermocline actually generated a 20% smaller hypolimnion volume.

The extra heat in the water column was apparently confined to the epilimnion, where changes were on the order of 4°C (Figure 7; only GFDL scenario results are shown). The waters of the hypolimnion increased 1–2°C, with an even greater increase of 3–4°C occurring later in the year. The

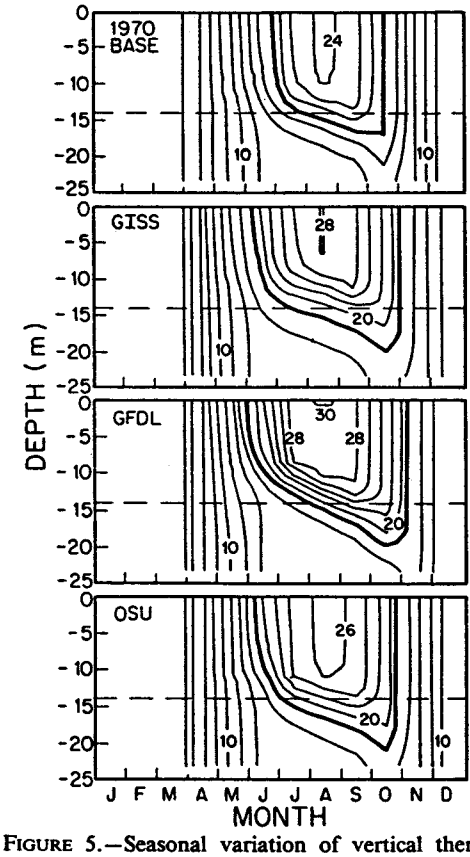

FIGURE 5.—Seasonal variation of vertical thermal structure in Lake Erie's central basin in 1970 (base) and for three warming scenarios (GISS, GFDL, OSU). Contours are in °C. Horizontal dashed lines mark the thermocline location from the base situation. The 18°C contour is darkened to facilitate comparison.

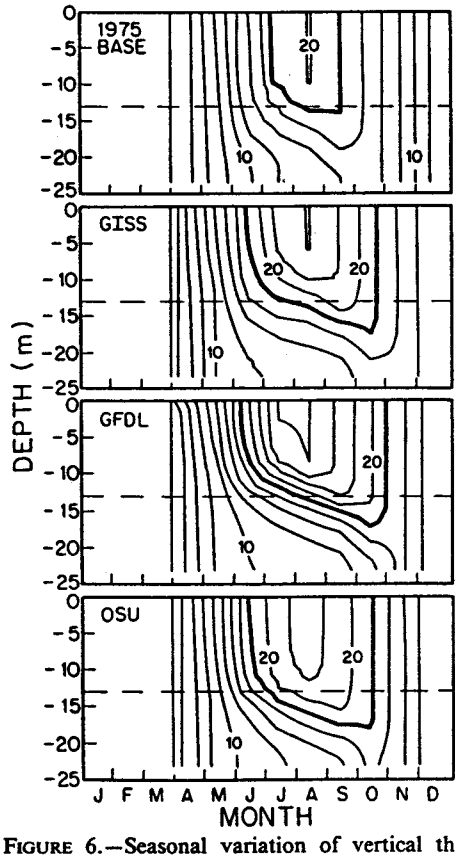

FIGURE 6.—Seasonal variation of vertical thermal structure in Lake Erie's central basin in 1975 (base) and for three warming scenarios (GISS, GFDL, OSU). Contours are in °C. Horizontal dashed lines mark the thermocline location from the base situation. The 18°C contour is darkened to facilitate comparison.

TABLE 1.—Hydrodynamic model predictions for the 1970 and 1975 base conditions, three warming scenarios (GISS, GFDL, OSU models) applied to each of those base years, and two scenarios of winds and heating used to examine the model's sensitivity to different forcing functions.

Simulation	Thermocline depth[a] (m)	Length of warming season[b]			Temperature maximum (°C)	Temperature difference[c] (°C)	Vertical dispersion[d] (cm^2/s)	Increase[e] in hypolimnion volume (%)
		Start	End	Duration (d)				
1970 base	14	Jun 23	Oct 14	113	25	9	0.02	
1975 base	13	Jul 10	Sep 12	64	20	5	0.12	
1970 GISS	10	Jun 5	Oct 31	148	28	10	0.02	90
1970 GFDL	12	May 30	Nov 5	159	30	12	0.02	50
1970 OSU	14	Jun 4	Oct 27	145	27	9	0.02	10
1975 GISS	10	Jun 14	Oct 20	128	24	7	0.06	40
1975 GFDL	11	May 31	Oct 31	153	27	11	0.07	30
1975 OSU	14	Jun 15	Oct 14	121	23	6	0.09	−20
1970 winds, 1975 heating	15	Jul 14	Sep 9	57	19			
1975 winds, 1970 heating	12	Jun 19	Oct 14	117	26			

[a] Based on depth of the maximum vertical temperature gradient during August.
[b] Based on presence of water with temperatures of 18°C or above at the surface.
[c] Based on averages over the epilimnion and the hypolimnion for August.
[d] Based on August values.
[e] Relative to base.

temperature difference across the epilimnion–hypolimnion interface, therefore, increased by 2–3°C (Table 1). Such a difference is certain to reduce the exchange between the upper and lower layers of the lake.

We conducted sensitivity evaluations to examine the base years with different combinations of forcing functions. For example, experiments were performed in which the 1970 winds were used in conjunction with the 1975 heating data and vice versa. The simulations showed that the location of the thermocline is a delicate balance between wind stirring and surface heating (Table 1). Stronger winds caused the thermocline to form later and deeper. Conversely, weaker winds or larger surface heating produced an earlier, shallower thermocline. These ideas were further substantiated by the differences between the OSU and GISS–GFDL results. Other experiments have been conducted to address the findings of Assel et al. (1985), who showed that, during very warm periods analogous to those under the doubled-CO_2

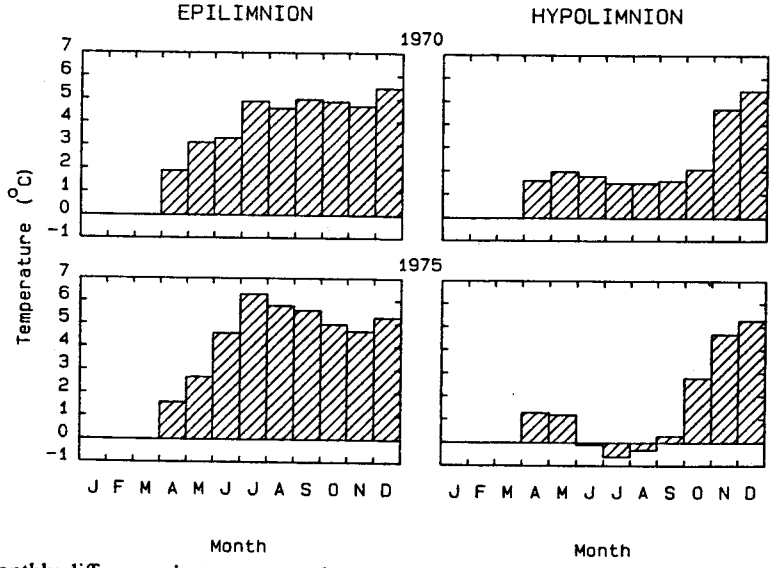

FIGURE 7.—Monthly differences in temperature between the GFDL warming scenario and 1970 and 1975 base conditions for the epilimnion and hypolimnion of Lake Erie's central basin.

scenarios, it is likely that the central basin of Lake Erie will be void of its characteristic winter ice cover. Results from simulations with initial temperature profiles of 4°C and 8°C indicated that the summer conditions for these experiments were identical to those of the benchmark evaluation, which used a 2°C initial profile.

Water Quality Response to Scenarios

During the calibration of the hydrodynamic model, we tolerated some variance between the model results and corresponding data because the climate scenarios were designed as sensitivity analyses and not as absolute predictions. The hydrodynamic model was used to compute the difference in thermal structure and thermocline depth between the base case and the scenario being investigated. These differences were incorporated into the previously calibrated eutrophication model (Di Toro and Connolly 1980) and new calculations for dissolved oxygen concentrations were conducted. The differences in dissolved oxygen between the base case and the scenario under investigation were recorded for use in the analyses of our study. Thus the absolute accuracy of the hydrodynamic model was not at issue. The question was whether the hydrodynamic model was capable of computing the differences in thermal structure and mixing for the different scenarios. The hydrodynamic model and, in particular, its vertical mixing submodel have been independently calibrated in the past for conditions that are more general than those specific to Lake Erie. Thus, it was reasonable to expect that the hydrodynamic model could compute reliable differences that depend much more strongly on the differences in the scenario-based forcing than on fine-tuned values generated for this particular application.

The water quality model was configured by use of the horizontal segmentation shown in Figure 1. The vertical segment boundary was chosen, logically, between the epilimnion and the hypolimnion, within the thermocline region. For consistency with Di Toro and Connolly (1980), the thickness of the epilimnion (H_e in Figure 1) was taken in the base years as 17 m for 1970 and 13 m in 1975. For the warming scenario simulations, the base-year thickness was changed by the difference in the calculated thermocline depth between the base year and the particular scenario under consideration (Table 1).

The temperature distributions computed by the hydrodynamic model were volume-averaged over the hypolimnion and inserted in equation (8) to produce the vertical dispersion coefficients. The dispersion coefficients computed from equation (8) that were consistent with the new August temperatures are shown in Table 1. The base year 1970 has small dispersion coefficients (0.02 cm^2/s) in August whereas 1975 has values six times larger (0.12 cm^2/s). This is due primarily to the rather large epilimnion–hypolimnion temperature difference in 1970 (9°C) versus that in 1975 (5°C). There was little scenario-to-scenario variation in the coefficients for the 1970-based situations. The temperature difference between the epilimnion and hypolimnion was great enough in the 1970-based situations to prevent mixing. On the other hand, the 1975-based situations showed much scenario-to-scenario variation. The increase in the temperature difference reduced the vertical exchange by a factor of 2 or so, from 0.09 cm^2/s to 0.06 cm^2/s, during times of maximum stratification.

The projected epilimnion and hypolimnion dissolved oxygen for the GFDL scenarios are shown on Figure 8 along with the observations for 1970 and 1975. The differences between the hatched and clear vertical bars in Figure 8 are the warming-induced changes. The projected values were obtained by adding the difference between those values computed by the doubling scenarios and the base scenarios to the original observations. Dissolved oxygen concentrations in the epilimnion worsened by about 1 mg/L in every instance. This decrease was primarily due to the change in the saturation concentration for dissolved oxygen. For example, a 4°C increase in epilimnion temperature produced an approximately 0.6-mg/L decrease in the concentration of dissolved oxygen. The hypolimnion dissolved oxygen (Figure 8) decreased dramatically; losses of 1–2 mg/L were typical under the various scenarios. The 1975-based situations, for which the observations did not reach the anoxic level, showed losses of up to 5 mg/L in dissolved oxygen. The 1970 observations showed very low levels of dissolved oxygen already, so a small loss led immediately to anoxia. The GISS scenario with 1970 as the base year led to a 3-month period of higher levels of dissolved oxygen.

The overall decrease in dissolved oxygen can be explained by noting that the sinks of oxygen in the hypolimnion (benthic respiration rate due to the decay of organic material and bacterial metabolism in the water column) were strong functions of temperature. The increase in hypolimnion temperatures due to climate warming consider-

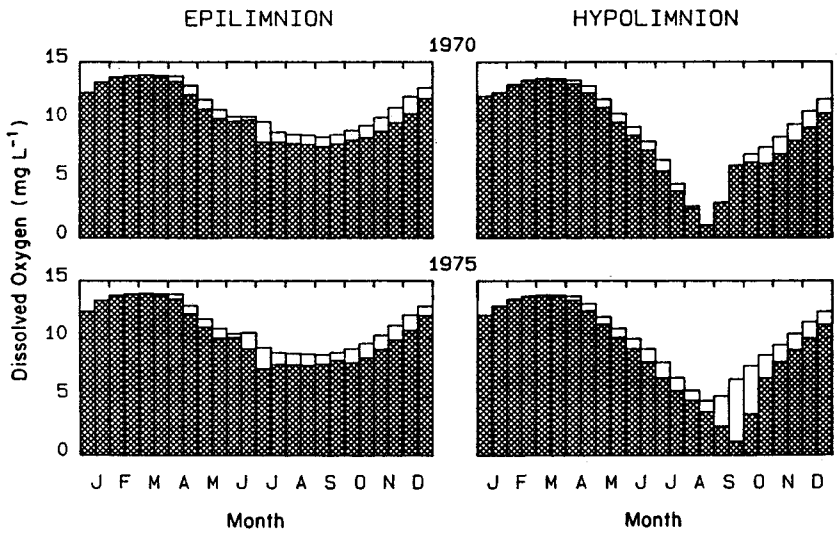

FIGURE 8.—Monthly averaged dissolved oxygen for the epilimnion and hypolimnion of Lake Erie's central basin for 1970 and 1975. Hatched bars denote the GFDL-based warming scenario projection; clear bars are observations.

ably increased the sediment oxygen demand, the largest of the oxygen sinks, overwhelming any decrease in dissolved oxygen saturation. On the other hand, the volume of the hypolimnion increased (Table 1) and there was a greater volumetric reservoir of dissolved oxygen available to meet water column and benthic oxygen demands. The results of the scenario simulations indicated that the volumetric depletion rate became greater despite increases in the volume of the hypolimnion. Such increases in the absence of any change in sediment oxygen demand would result in a smaller volumetric depletion rate and high levels of dissolved oxygen. Figure 9 illustrates the volumetric depletion rates for the model scenarios and the base cases. An experiment wherein the thermal structure of the 1970-based GFDL scenario was used in conjunction with the observed, and somewhat cooler, 1970 temperatures showed that high levels of dissolved oxygen would be present. This suggested that the major decline in the lake's water quality was due to warmer lake temperatures, which increased the rate of bacterial activity in the sediment enough to produce apparently significant increases in sediment oxygen demand. The OSU scenario produced the worse dissolved oxygen distributions because the thermocline depth changed little while the sediment oxygen demand became much greater, again due to elevated temperatures. It appears that no matter at what depth the thermocline forms, increased lake temperatures would lead to degraded water quality.

The change in the areal extent of anoxia, defined here as 0 mg/L, in the central basin was computed with the empirical method developed by Di Toro and Connolly (1980). Monthly averages of the percentage of the central basin that observationally was anoxic and the percentage that was projected to become anoxic under each of the scenarios is provided in Table 2. The 1970-based scenarios produced areas of anoxia that encompassed considerable portions of the lake. The areas of anoxia also occurred 2 weeks or so sooner than in the base case. The 1970 observations indicated only 1 month of severe anoxia occurred and that only about 41% of the basin was affected. The OSU scenario, with the smallest change in air temperature, produced the worst estimate in terms of extra anoxia for both the 1970 and 1975 base simulations. It should be remembered that 1975 had ample dissolved oxygen, yet with climate warming both the GFDL and OSU scenarios showed regions of anoxia when based on that year.

Summation

An analysis of the results from the coupled model forced by the climate-warming scenarios and specifically designed sensitivity experiments suggested that a doubling of atmospheric CO_2 will cause a substantial decline in Lake Erie's water quality. The modeled decline was due to the expected warmer lake temperatures, which would increase the rate of bacterial activity in the hypolimnion waters and sediment enough to drive

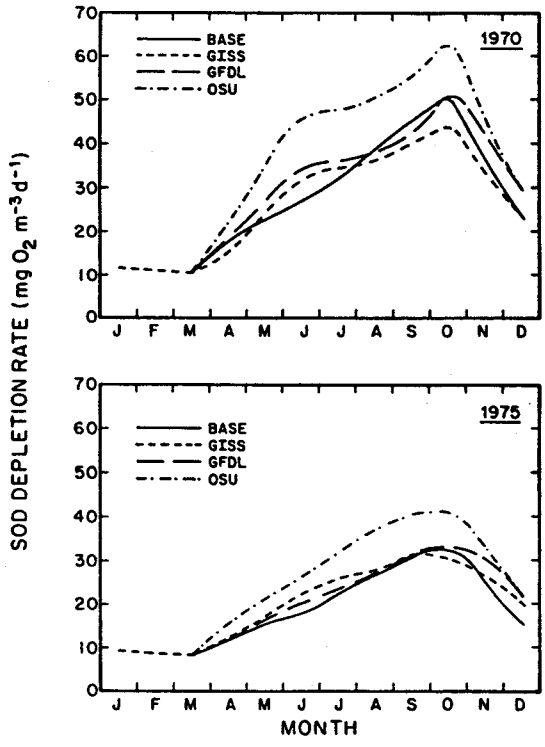

FIGURE 9.—Annual cycle in Lake Erie's central basin of the volumetric hypolimnion sediment oxygen demand (SOD) from base conditions in 1970 and 1975 and three warming scenarios (GISS, GFDL, OSU).

the system to lower dissolved oxygen concentrations. Such decline was independent of the depth at which the thermocline became established. Water quality criteria for ambient dissolved oxygen for "coldwater" fish in fresh water specify a 1-d minimum of 3.0 mg/L for adult life stages and 8.0 mg/L for early life stages (USEPA 1985). The 1-mg/L reduction of epilimnion dissolved oxygen that was projected by all warming scenarios would not greatly affect fish life. However, the projected declines of dissolved oxygen in the hypolimnion could lead to concentrations of 3 mg/L or less, which would certainly pose a threat to adult fish life (Cohen 1986).

Our conclusions must be tempered with the following caveats. First, it is possible that the eutrophication model was exercised beyond the range of data (specifically water temperatures) for which it was calibrated and validated. This leads to increased uncertainty in the magnitude of the results for the various climate-warming scenarios, but should not affect the direction of change. In addition, the conclusions apply to the central basin

TABLE 2.—Monthly average areal percentages of anoxia in Lake Erie's central basin for the base years 1970 and 1975 and the projections from three warming scenarios (GISS, GFDL, OSU).

Condition	1970		1975, Aug
	Jul	Aug	
base	10	41	0
GISS	12	80	0
GFDL	23	94	6
OSU	55	100	29

of Lake Erie only. The eastern basin is much deeper and the western basin is much shallower, so both are certain to respond differently to climate warming. Indeed, some caution should be exercised in attempts to extend the conclusions of this study to the Great Lakes in general. Dissolved oxygen concentrations in lakes are very dependent on site-specific characteristics such as morphometry, prevailing wind conditions, nutrient enrichment, light extinction, and the time history of external loadings, as reflected in the composition of the sediments. Although it is true in general that dissolved oxygen depletion rates should increase with increasing temperature, site-specific studies like ours will probably be necessary to develop actual predictions for a particular lake.

Although the two base years encompass a wide range of baseline anoxic conditions, they do not represent a full range of climate variability. No change is assumed in nutrient loadings from the base years and the analysis does not incorporate the estimated expected drop in lake levels associated with climatic warming (Cohen 1987). Lower lake levels may reduce the volume of the lower layer in Lake Erie, increasing eutrophication. The models were not run for winter, but the sensitivity of results to higher water column temperatures in the spring was tested, and no significant difference resulted.

In future efforts, it may be possible to estimate the reductions in the total phosphorus loading that would be required to return the lake to its present conditions. However, simulations of at least 5 years must be made with the water quality model so that the long-term response of the sediment can be properly incorporated. These simulations, once conducted, can be analyzed to establish target loadings for phosphorus that would eliminate the anoxia in the central basin.

Acknowledgments

The thoughtful stewardship and invaluable technical contributions of Joel B. Smith of the

U.S. Environmental Protection Agency (USEPA) are gratefully acknowledged. This manuscript benefitted greatly from the comments of John Paul, also of the USEPA. We thank Barbara J. Grehl for making many of the computer simulations and for organizing the outputs in a manner that facilitated analysis, and Laurie Davanzo and Barbara Grier for their help in the preparation of this paper. The study was funded by the USEPA under contract 68-01-7288. It does not necessarily reflect the Agency's views, and no official endorsement should be inferred from it.

References

Assel, R. A., C. R. Snider, and R. Lawrence. 1985. Comparison of 1983 Great Lakes winter weather and ice conditions with previous years. Monthly Weather Review 113:291–303.

Bierman, V. J. 1976. Mathematical model of the selective enhancement of blue-green algae by nutrient enrichment. Pages 1–32 *in* R. Canale, editor. Modeling biochemical processes in aquatic ecosystems. Ann Arbor Science, Ann Arbor, Michigan.

Blumberg, A. F., and G. L. Mellor. 1983. Diagnostic and prognostic numerical circulation studies of the South Atlantic Bight. Journal of Geophysical Research 88:4579–4592.

Blumberg, A. F., and G. L. Mellor. 1987. A description of a three-dimensional coastal ocean circulation model. Pages 1–16 *in* N. S. Heaps, editor. Three-dimensional coastal ocean models. American Geophysical Union, Washington, D.C.

Cohen, S. J. 1986. Impacts of CO_2-induced climatic change on water resources in the Great Lakes basin. Climatic Change 8:135–153.

Cohen, S. J. 1987. Influences of past and future climates on the Great Lakes region of North America. Water International 12:163–169.

De Pinto, J. V., T. C. Young, and D. K. Salisbury. 1986. Impact of phosphorus availability on modeling phytoplankton dynamics. Hydrobiological Bulletin 20:225–243.

Derecki, J. A. 1976. Heat storage and advection in Lake Erie. Water Resources Research 12:1144–1150.

Di Toro, D. M. 1980. The effect of phosphorus loadings on dissolved oxygen in Lake Erie. Pages 191–205 *in* R. C. Loehr, C. S. Martin, and W. Rast, editors. Phosphorus management strategies for lakes. Ann Arbor Science, Ann Arbor, Michigan.

Di Toro, D. M., and J. P. Connolly. 1980. Mathematical models of water quality in large lakes. Part 2: Lake Erie. U.S. Environmental Protection Agency, Report EPA-600/3-80-065, Duluth, Minnesota.

Di Toro, D. M., N. A. Thomas, C. E. Herdendorf, R. P. Winfield, and J. P. Connolly. 1987. A post audit of a Lake Erie eutrophication model. Journal of Great Lakes Research 13:801–825.

Galperin, B., L. H. Kantha, S. Hassid and A. Rosati. 1988. A quasi-equilibrium turbulent energy model for geophysical flows. Journal of the Atmospheric Sciences 45:55–62.

Gill, A. E. 1982. Atmosphere–ocean dynamics. Academic Press, New York.

Haney, R. L. 1971. Surface thermal boundary conditions for ocean circulation models. Journal of Physical Oceanography 1:241–248.

Hansen, J., and seven coauthors. 1984. Climate sensitivity: analysis of feedback mechanisms. Geophysical Monograph, American Geophysical Union 29:130–163.

Heinrich, J., W. Lick, and J. Paul. 1981. Temperatures and currents in a stratified lake: a two-dimensional analysis. Journal of Great Lakes Research 7:264–275.

IJC (International Joint Commission). 1978. Great Lakes water quality agreement of 1978, Washington, D.C. and Ottawa, November 22, 1978. IJC, Windsor, Ontario.

Kraus, E. B. 1977. Modelling and prediction of the upper layers of the ocean. Pergamon Press, New York.

Lam, D. C. L., and W. M. Schertzer. 1987. Lake Erie thermocline model results: comparison with 1967–1982 data and relation to anoxic occurrences. Journal of Great Lakes Research 13:757–769.

Lam, D. C. L., W. M. Schertzer, and A. S. Fraser. 1983. Simulation of Lake Erie water quality responses to loading and weather variations. National Water Research Institute, Inland Waters Directorate Scientific Series 134, Burlington, Ontario.

Large, W. G., and S. Pond. 1981. Open ocean momentum flux measurements in moderate to strong winds. Journal of Physical Oceanography 11:324–336.

Manabe, S., and R. T. Wetherald. 1986. Reduction in summer soil wetness induced by an increase in atmospheric carbon dioxide. Science (Washington, D.C.) 232:626–628.

Martin, P. J. 1985. Simulation of the mixed layer at OWS November and Papa with several models. Journal of Geophysical Research 90:903–916.

McCormick, M. J., and G. A. Meadows. 1988. An intercomparison of four mixed layer models in a shallow inland sea. Journal of Geophysical Research 93:6774–6788.

Mellor, G. L., and T. Yamada. 1982. Development of a turbulence closure model for geophysical fluid problems. Reviews of Geophysics and Space Physics 20:851–875.

Schertzer, W. M. 1987. Heat balance and heat storage estimates for Lake Erie, 1967 to 1982. Journal of Great Lakes Research 13:454–467.

Schlesinger, M. E., and J. F. B. Mitchell. 1987. Climate model simulations of the equilibrium climatic response to increased carbon dioxide. Reviews of Geophysics 25:760–798.

Schlesinger, M. E., and Z.-C. Zhao. 1988. Seasonal climate changes induced by doubled CO_2 as simulated by the OSU atmospheric GCM/mixed-layer ocean model. Climate Research Institute Report, Oregon State University, Corvallis, Oregon.

Schwab, D. J. 1978. Simulation and forecasting of Lake Erie storm surges. Monthly Weather Review 94: 1476–1487.

Schwab, D. J., and J. A. Morton. 1984. Estimation of overlake wind speed from overland wind speed: a comparison of three methods. Journal of Great Lakes Research 10:68–72.

Thomann, R. V., D. M. Di Toro, R. Winfield, and D. J. O'Connor. 1975. Mathematical modeling of phytoplankton in Lake Ontario, 1. Model development and verification. U.S. Environmental Protection Agency, EPA 660/3-75-005, Corvallis, Oregon.

USEPA (U.S. Environmental Protection Agency). 1985. Ambient water quality criterion for dissolved oxygen: freshwater aquatic life. Federal Register 50: 15634–15668.

Vollenweider, R. A., W. Rast, and J. Kerekes. 1980. Phosphorus loading concept and Great Lakes eutrophication. Pages 207–234 *in* R. C. Loehr, C. S. Martin, and W. Rast, editors. Phosphorus management strategies for lakes. Ann Arbor Science, Ann Arbor, Michigan.